Some like it hot: efficiency of the type III secretion system has multiple thermosensitive behaviors in the *Pseudomonas syringae* complex

E. Caullireau[a,b,*], D. Danzi[a], V.M. Tempo[a], M. Pandolfo[a], C.E. Morris[b], E. Vandelle[a#]

[a] Dipartimento di Biotecnologie, Università degli Studi di Verona, I-37134 Verona, Italia.

[b] INRAE, Pathologie Végétale, F-84140, Montfavet, France.

Corresponding author: Elodie Vandelle, elodiegenevieve.vandelle@univr.it

* Present address: School of Biological Sciences, University of Utah, Salt Lake City, UT 84112, USA.

Keywords: bacterial virulence, T3SS, hypersensitive response, molecular plant-pathogen interactions, environmental factors

Word count: 6079

Summary

The *Pseudomonas syringae* complex is an important group of ubiquitous bacteria containing plant pathogenic strains of which many cause damage and economic losses to a wide range of crops. Efforts to elucidate the determinants of host range have focused on the repertoires of effectors in the Type 3 Secretion System (T3SS). However, recently, we showed that the inability

of a *P. syringae* pv. *actinidiae* strain to trigger an hypersensitive response (HR) in *A. thaliana* is due to an inefficient T3SS and not to the absence of a recognized effector. In this context, we compared the efficiency of the T3SS of several *P. syringae* strains belonging to different phylogroups. Through statistical analysis, we assessed the temporal dynamics of the induction of ion leakage, an HR indicator, in *A. thaliana*. We revealed that *Pto*DC3000 *avrB* and *Pma*M6 *avrB* consistently triggered a strong HR while other strains induced it at significantly different intensities depending on temperature. Among thermosensitive strains, both low and warm temperature-dependencies for T3SS efficiency were observed, irrespective of the *in-vitro* growth optimum of the strains. Surprisingly, differences were also observed among quasi-clonal strains. These results reveal a strong, strain-specific regulatory role of temperature in effector injection and reinforce the importance of environmental factors in the outcome of plant-bacteria interactions. Moreover, this work highlights the need to study bacterial virulence for a broader set of strains beyond model strains, such as *Pto*DC3000, that are not representative of the whole *P. syringae* complex.

Introduction

Pseudomonas syringae is a complex of gram-negative bacteria that poses a threat to global agriculture with new outbreaks that emerge regularly (Lamichhane et al., 2014; Lamichhane et al., 2015). *P. syringae* has been divided into at least 13 phylogenetic groups (phylogroups, PG), further divided into 23 clades (Berge et al., 2014). During the infection, *P. syringae* relies on an arsenal of virulence factors, though its pathogenesis is predominantly mediated by the type III secretion system (T3SS), a highly conserved needle-like specialized protein secretion machinery,

45 found in numerous gram-negative bacterial pathogens affecting plants and animals. T3SS forms
46 a continuous channel, guiding the translocation of diverse proteinaceous effectors (T3Es)
47 directly into the host cell or apoplast (Büttner and He, 2009; Jin and He, 2001; Li, 2002; Roine et
48 al., 1997). *P. syringae* strains with the canonical T3SS commonly harbor a repertoire of
49 approximately 15-30 T3SEs, which facilitate the invasion of plant host cells, suppress plant
50 immunity, or interfere with essential plant cellular processes (Chang et al., 2005; Cunnac et al.,
51 2009; Galán and Collmer, 1999; Guo et al., 2009; Guttman et al., 2002; Hueck, 1998; Lee, 1997;
52 Lindeberg et al., 2012; Martel et al., 2022; Mudgett and Staskawicz, 1998; Xin et al., 2016). Of
53 note, there is no direct relationship between the size or content of the T3SE repertoire and host
54 range (Baltrus et al., 2017; Morris et al., 2019).
55 According to the 'disease triangle' paradigm (Stevens, 1960), plant diseases arise from the
56 interplay between a susceptible plant and a virulent pathogen, under conducive environmental
57 conditions, resulting in a compatible reaction. Overall plant-pathogen interaction mechanisms
58 are highly influenced by environmental conditions, which can either favor, have neutral effects,
59 or hinder both partners (Velásquez et al., 2018; Xin et al., 2018). Among the environmental
60 factors, temperature has a regulatory role for virulence in plant-associated bacteria (reviewed in
61 references Smirnova et al., 2001; Velásquez et al., 2018).
62 Within the *P. syringae* species complex, temperature variations impact various traits crucial for
63 bacterial fitness, including phytotoxin expression, exopolysaccharide biosynthesis, motility or
64 the quorum-sensing system (Aguilera et al., 2007; Aguilera et al., 2017; Arvizu-Gómez et al.,
65 2013; Bender et al., 1999; Braun et al., 2009; Hockett et al., 2013; Krishna et al., 2022; Li et al.,
66 2006; Nüske and Fritsche, 1989; Palmer and Bender, 1993; Peñaloza-Vázquez et al., 1997;

67 Scalschi et al., 2022; Smirnova et al., 2001; Ullrich et al., 2000; Weingart et al., 2004). T3SS has
68 also been investigated concerning its possible thermoregulation. In *P. syringae* pvs. *syringae* and
69 *tomato*, the secretion of HopPsyA and AvrPto effectors *in vitro* was impaired at temperatures
70 above 22°C and 20°C, indicating some kind of low-temperature-dependency for their T3SS
71 efficiency (Van Dijk et al., 1999). In contrast, recent findings in *Pto* DC3000 revealed that the
72 translocation of T3Es in *A. thaliana* cells is enhanced at 30°C compared to 23°C, indicating the
73 possible T3SS efficiency even at elevated temperatures (Huot et al., 2017). However, in tomato,
74 the expression of T3SS-related genes *hrpL* and *hrpA* in this same strain was not affected by a
75 temperature rise from 26°C to 31°C, although the expression of the avirulence gene *avrPtoB* was
76 significantly reduced (Scalschi et al., 2022). On the other hand, for *P. syringae* pv. *actinidiae*
77 strains, it was shown that there was no difference in *hrpA1* promoter activity *in vitro* across a
78 temperature range of 18-28°C, nonetheless, substantial differences were evident at a functional
79 level, demonstrating a low-temperature-dependency for T3SS efficiency for these strains (Puttilli
80 et al., 2022). However, the complete implications of warm temperatures on *P. syringae* virulence
81 in plants remain poorly understood (Hockett et al., 2013; Li et al., 2006). Studies indicate
82 complex interactions with plant immune signaling pathways, emphasizing the need for further
83 research to understand their implications in terms of disease (Cheng et al., 2013; Huot et al.,
84 2017).
85 Evidence of the influence of temperature in regulating virulence factors in *P. syringae* species
86 complex has been documented, however, there have not been studies dedicated to comparing
87 strains under identical conditions. Consequently, we wanted to further understand the role of
88 the temperature on the function/activation dynamics of the T3SS by investigating a broader

89 range of diversity within the *P. syringae* species complex under comparable conditions. For this
90 purpose, we transformed 13 strains of *P. syringae* in phylogroups 1, 2 and 3 to carry the effector
91 AvrB and infiltrated them into *Arabidopsis thaliana* Col-0 leaf disks. In this model plant, AvrB is
92 indirectly recognized by the resistance protein RPM1, through RIN4 modification, which triggers
93 HR (Innes et al., 1993; Mackey et al., 2002; Mudgett, 2005). Infiltrated leaf disks were incubated
94 at different temperatures and the quantification of electrolyte leakage served as the indicator of
95 HR onset. Conductivity increase was used as a proxy for T3SS efficiency, and this allowed us (i) to
96 effectively discriminate strains based on a robust phenotype directly linked to the activation of
97 the T3SS, and (ii) to observe different behaviors in response to temperature.
98

99 ## Results

100 **The intensity of HR induction is not strictly reproducible for individual strains.**

101 To evaluate T3SS functionality at different temperatures, *avrB*-expressing *P. syringae* strains were
102 infiltrated into *A. thaliana* Col-0 leaf disks. As a T3SS-dependent mechanism, HR was quantified
103 by measuring the increase in ion leakage due to dying cells. Conductivity levels measured among
104 the diverse replicated experiments were highly variable. The conductivity levels measured for a
105 given modality (*i.e.*, one strain infiltrated and incubated at one temperature) doubled or tripled
106 among replicated experiments. Four examples of this variability are shown in Figure 1. For
107 instance, across the seven replicated experiments for strain USA007 *avrB* at 18°C, the ratio of
108 areas under the curves calculated between the one that induced the most and the least was
109 equal to 2.8 (Figure 1b). Moreover, conductivity showed considerable heteroscedasticity, *i.e.*
110 there was a positive correlation between the mean area under the curves and their variance

111 with Spearman's coefficient = 0.91; $p < 0.05$ (Figure S1). This large variability raised the question
112 of how to quantify HR induction to compare the strains, as addressed in the next section.
113
114 **The intensity of HR induction varies among strains.**
115 To compare HR induction intensity among strains, we accounted for the variability described
116 above by fitting Linear Mixed effects Models to our data. This statistical approach allowed us to
117 classify strains as inducers or non-inducers at each of the temperatures that we tested. This
118 revealed that almost all the *P. syringae* strains induced HR except for J35 *avrB* at all the
119 temperatures, MAFF302273 *avrB* at 24°C and 28°C, B728a *avrB* at 24°C, and 1448A *avrB* and
120 CRA-FRU 8.43 *avrB* at 28°C (Table 1). The inducer strains led to conductivity levels that were
121 significantly greater than those measured in the mock treatment (10mM $MgCl_2$ or *hrp*-inducing
122 medium, HIM) ($p < 0.05$) according to Linear Mixed-effects Models. More specifically, our results
123 demonstrated that all the inducer strains varied in the intensity of the HR induction they caused.
124 The model estimated the mean difference in points of conductivity measured between the
125 tested modality and the mock treatment. The values presented in Table 1 ("Estimate") are
126 proxies of the intensity of HR induction for each strain. DC3000 *avrB* and M6 *avrB* displayed the
127 highest values ("Estimate" > 65 regardless of the temperature tested), whereas some others
128 such as the three quasi-clonal strains CC0073 *avrB*, CC0094 *avrB* and CC1498 *avrB* averaged less
129 than 20. These differences are also reflected in the mean areas under conductivity progress
130 curves (AUCPC) at each temperature as shown in Figure 2. This proxy of the HR induction
131 intensity was correlated neither with the *avrB* expression levels (Figure S2) nor with the bacterial
132 growth capacity at a given temperature (Figure S3).

133

134 **The intensity of HR induction is temperature-sensitive in half of the inducer strains.**

135 With Linear Mixed-effects Models (LMM), we categorized the HR inducer strains according to
136 the temperature-sensitivity of HR induction. Six out of eleven HR inducer strains were insensitive
137 to a change in temperature (DC3000 *avrB*, M6 *avrB*, LAB0041 *avrB*, CC0073 *avrB*, 1448A *avrB*) (p
138 > 0.05) (Table 1). The other HR inducer strains were temperature-sensitive based on LMM
139 analyses ($p < 0.05$) and could be categorized into two groups according to whether the
140 "Estimate" values were negative or positive. In one group, strains showed higher conductivity
141 with lower temperatures (T1 *avrB*, CRA-FRU 8.43 *avrB* and USA007 *avrB*). In the case of CRA-FRU
142 8.43 *avrB* strain, the decrease in conductivity observed with increasing temperature led the
143 strain to be categorized as a non-inducer at 28°C (Table 1). In the other group, strains showed
144 higher conductivity with higher temperatures (CC0094 *avrB*, CC1498 *avrB* and B728a *avrB*).
145 Temperature-sensitivity of the *avrB*-expressing strains was further confirmed by the analysis of
146 HrpZ secretion *in vitro* as an assessment of T3SS functionality (Figure 3).

147

148 **The natural genomic background of the WT strains does not change the temperature**
149 **responsiveness patterns observed with *avrB*-expressing strains.**

150 Keeping in mind that the elicitation of the HR by AvrB could be subjected to a variety of factors,
151 including the action of other effectors, both in terms of host responses and competition for delivery by
152 the T3SS, we verified the functionality of the T3SS in vitro, assessing the secretion of the HrpZ protein.
153 While HrpZ detection for J35 *avrB* was consistent with its categorization as an HR non-inducer,
154 strain MAFF302273 *avrB* displayed a functional T3SS at all tested temperatures (Figure 3). Since

155 this strain constantly did not lead to conductivity increase once infiltrated into leaf disks, this
156 may suggest that MAFF302273 contains in its repertoire some suppressive effector(s) blocking
157 the ability of AvrB to trigger the HR in *A. thaliana*. Consequently, we established the effector
158 repertoire composition of all the strains by collecting information already available in the
159 literature for 10 strains and by performing effector prediction in silico for 3 others, following the
160 procedure reported previously (Dillon et al., 2019; Laflamme et al., 2020). However, to the best
161 of our knowledge, no evidence of direct or indirect antagonism between AvrB and other
162 effectors naturally present was found in any of the strains (Table S2). Furthermore, we
163 accounted for the outcome resulting from the interaction between *A. thaliana* Col-0 and our
164 subset of strains in their WT version. Firstly, many of them do not result in HR induction, due to
165 compatible interaction (DC3000, M6) or non-host incompatible interaction without HR (CRA-FRU
166 8.43, B728a, 1448A), hence justifying the need to introduce *avrB* to study T3SS efficiency with
167 this proxy (Table S3). On the other hand, the presence of *avrB* does not necessarily modify the
168 behavior of the strain. For instance, CC0094 WT induced HR in *A. thaliana* Col-0, displaying the
169 same warm-temperature dependency as observed with the *avrB*-expressing strain (Figure S4a).
170 Likewise, the low-temperature dependency behavior of CRA-FRU 8.43 was conserved across
171 both strain genotypes (with or without *avrB*) in the resistant *Actinidia arguta* (non-host plant
172 inducing effector-mediated HR with strains belonging to the same biovar 3; Figure S4b; Table
173 S3). Altogether, these findings demonstrate that although the HR induction by AvrB in our
174 experiment does not take place in isolation from the background of both interaction partners,
175 the various outcome scenarios with the WT strains allow us to support our conclusions made
176 with the *avrB*-expressing strains, hence confirming the robustness of our approach.

177

178 **Temperature-responsiveness patterns vary among strains with trends that are consistent**
179 **within a given phylogroup.**

180 A given phylogroup could contain strains that induced HR in temperature-sensitive and
181 temperature-insensitive ways (Table 1). However, the trend in temperature sensitivity was
182 constant withing a phylogroup among its temperature-sensitive strains. Indeed, the group of
183 strains whose T3SS was more efficient at lower temperatures and the group whose T3SS was
184 more efficient at higher temperatures belong to the phylogroups 1 and 2d, respectively (Table
185 1). Nevertheless, dramatic differences among strains even those that are very closely related
186 phylogenetically, were still observed as illustrated by the three quasi-clonal *avrB*-expressing
187 strains from phylogroup 2d, CC0073, CC0094 and CC1498 (Table 1) (Figure 4). CC0073 *avrB* was
188 temperature-independent in its ability to induce HR, while CC0094 *avrB* and CC1498 *avrB* both
189 showed clearly greater capacity at warmer temperatures. Moreover, in terms of intensity, the
190 inoculation with CC1498 *avrB* led to higher values of conductivity measured at 24 hpi than
191 CC0073 *avrB* and CC0094 *avrB*. Finally, in terms of kinetics, CC0073 *avrB* was responsible for a
192 faster HR induction at the beginning of the interaction that stalled – no matter the temperature–
193 , whereas CC0094 *avrB* and CC1498 *avrB* were much slower in inducing HR (Figure 4).

194

195 **Strains from the *P. syringae* complex display diverse speeds of HR induction.**

196 To account for dynamic aspects in the behaviors of *avrB*-expressing *P. syringae* strains, the time
197 point when half of the total ions (*i.e.* final conductivity value measured at 24 hpi) has leaked was
198 calculated for each replicated experiment for all modalities that were found to be HR-inducing.

199 We used this parameter – $hpi_{50\%}$ – as the indicator of HR induction velocity. An analysis of
200 variance of these ratios revealed significant differences among *avrB*-expressing strains (ANOVA1,
201 $p < 0.05$). DC3000 *avrB* and M6 *avrB* proved to be the fastest HR inducers with half of their total
202 induction already observable before 5 hpi (Figure 5a). Yet again, the diversity of behaviors within
203 phylogroups was revealed, even among the three *avrB*-expressing quasi-clonal strains (Figure 5,
204 post-hoc Dunn's test showed that CC0073 *avrB* and CC0094 *avrB* and CC1498 *avrB* groups
205 differed significantly at $p < 0.05$). Furthermore, $hpi_{50\%}$ values were compared across the different
206 temperatures overall revealing that higher temperatures correlated with faster electrolyte
207 leakage, consistent with the results observed for bacterial *in-vitro* growth (Figure 5b).
208

209 ## Discussion

210 **New perspectives on virulence thermoregulation processes.**

211 The diverse behaviors of T3SS efficiency observed in relation to incubation temperature indicate
212 that *P. syringae* has a very diverse adaptive potential for causing disease in the face of various
213 temperatures. This observation is another piece of evidence out of the many reported over the
214 past 30 years regarding the role of temperature in virulence regulation in plant-associated
215 bacteria (reviewed in references Smirnova et al., 2001; Velásquez et al., 2018). Our work has
216 presented new examples of relatively warm-temperature dependency for virulence efficiency,
217 consistent with previous findings about gene expression beyond and within the *P. syringae*
218 species complex (Czajkowski et al., 2017; Huot et al., 2017; Krishna et al., 2022; Peñaloza-
219 Vázquez et al., 1997; Wei et al., 2008; Wei et al., 2010). Altogether, these pieces of evidence
220 contradict the long-standing notions that, firstly, "almost all virulence genes of plant pathogenic

221 bacteria [...] exhibit increased transcription at temperatures well-below the respective growth
222 optima" (Smirnova et al., 2001) and, secondly, that "the increase of bacterial growth in plants at
223 elevated temperature cannot be explained by variations in intrinsic bacterial growth rate or
224 secretion of effector proteins at different temperatures" (Wang et al., 2009). Our findings
225 support a distinctly different perspective that aligns with more recent articles that present an
226 updated framework (Huot et al., 2017; Tribelli and López, 2022; Velásquez et al., 2018).
227
228 **Effector repertoire contribution in HR induction.**
229 Although *avrB* expression was assessed for all the strains, two of them (J35 *avrB* and
230 MAFF302273 *avrB*) were categorized as non-inducers for at least two of the tested
231 temperatures. The lack of HR induction could result from T3SS inactivation in *A. thaliana*,
232 potentially because of a quick PTI onset (Crabill et al., 2010). On the other hand, it could also be
233 a matter of speed of ETI onset, whose rapidity prevents cell death occurrence (Künstler et al.,
234 2016). Otherwise, it may be due to the presence in the repertoire of the strain of some
235 suppressive effector(s) (Jamir et al., 2004), or some effector(s) targeting a molecular actor
236 involved in both PTI and ETI, or simply blocking the PTI – required in the first place for ETI
237 activation (Ngou et al., 2021). Although our analysis of effector repertoire composition (PsyTEC;
238 Laflamme et al., 2020) did not allow to identify one single or group of effectors antagonistic to
239 AvrB, we cannot rule out the occurrence of 'meta-effector' interactions (Kubori et al., 2010;
240 Martel et al., 2022). Overall, the in-depth-study of the effector repertoires of all the strains used
241 in our work could help to explain the differences observed in terms of HR intensity, with one or

242 more effectors that may inhibit HR but also enhance it conversely – as observed for strain
243 CC1498 *avrB* versus strain CC0094 *avrB*, for example.
244
245 **Temperature and plant immunity.**
246 Using HR induction as a proxy for T3SS efficiency, we implicitly accounted for plant defense
247 mechanisms that play a role in the response (Künstler et al., 2016). In *A. thaliana*, the role of
248 temperature in plant immunity is more complex than reported by previous studies. In 2009,
249 Wang and colleagues concluded that a mild increase in temperature impaired both PTI and ETI,
250 suggesting a general deficiency in the plant defense system at elevated temperatures (28-30°C)
251 (Wang et al., 2009). Subsequently, a straightforward dichotomy was established: less efficient
252 ETI (effective from 10 to 23°C, with a peak at 18°C) versus more efficient PTI (effective from 23
253 to 32°C, with a peak at 28°C) as the temperature increases (Cheng et al., 2013). This model was
254 later validated by the demonstration that, since ETI relies on distinct processes (*i.e.*, virulence
255 suppression and programmed cell death/HR), only HR was inhibited by elevated temperatures as
256 the virulence suppression was maintained (Menna et al., 2015). However, despite their
257 demonstration that ion leakage from *A. thaliana* leaf disks infiltrated with the avirulent DC3000
258 strain is completely inhibited at 28°C-30°C, our results for this *avrB*-expressing strain and CC0094
259 *qvrB* and CC1498 a*vrB* contradict this finding.
260 Temperature variations may affect the kinetics of effector translocation and/or binding to their
261 targets and hence impact the speed and efficiency of signaling cascades involved in the defense
262 response. Comparison of the time point when half of the final conductivity measured at 24 hpi –
263 $hpi_{50\%}$ – among temperatures for a given HR-inducer strain revealed that the elevation of the

264 temperature led to an acceleration of electrolyte leakage as temperature increased. As this
265 observation was maintained across the strains that induced HR at different temperatures, it is
266 tempting to associate this general effect of accelerated response with the effect of the higher
267 temperature on the plant, and not on the T3SS activation or efficiency. Nevertheless, across all
268 strains, we demonstrated that some were faster than others to induce HR, also indicating some
269 pathosystem-specific behaviors.
270
271 **Temperature and effector secretion properties.**
272 Interestingly, a few examples of temperature-dependency for T3E secretion have been shown to
273 be 'protein/effector specific' – mentioning some specific secretion properties of AvrB (Van Dijk
274 et al., 1999). Likewise, the two avirulent DC3000 strains with which HR suppression at elevated
275 temperatures was demonstrated carried either the HopZ1a or AvrRpt2 effector (Menna et al.,
276 2015). HopZ1a, AvrRpt2 and AvrB are recognized by the NLRs ZAR1, RPS2 and RPM1,
277 respectively, which are all members of the subgroup of CC-NLRs. The unclear variability of
278 temperature-sensitivity across different NLR subgroups (CC-NLRs versus TIR-NLRs) (Hua, 2014;
279 Menna et al., 2015) suggests that sensitivity may not be conserved in all NLRs or CC-NLRs, given
280 their distinct structural and functional properties. In this light, it is reasonable to attribute the
281 differences observed between our work and the one of Menna and colleagues (Menna et al.,
282 2015) to the different 'ligand-receptor' couples used. Echoing the differences in 'protein/effector
283 specific' secretion efficiency, there are likely to be differences in temperature-sensitivity for
284 effector recognition by R proteins, providing strong support to our choice to introduce the same
285 effector in all strains to ensure a proper comparison of HR induction dynamics. Overall, we

286 assume that the impact of temperature on T3SS-secretion/ETI/HR-triggering efficiencies can be
287 highly pathosystem-specific.
288
289 **Virulence thermoregulation in relation to disease development.**
290 Since various virulence factors may be controlled by the same thermoregulation components
291 (Klinkert and Narberhaus, 2009; Smirnova et al., 2001), one intriguing question is whether the
292 effect of temperature on virulence factors is consistent (i) for a given strain, and (ii) with
293 temperature conditions at which disease occurrence is generally reported. In other words, do
294 our results correspond to what is known about disease epidemiology under field conditions? For
295 *P. syringae* pv. *phaseolicola*, low-temperature-dependency was established for phaseolotoxin
296 production and T6SS regulation, in line with the development of halo blight of bean favored at
297 temperatures below 25°C (Goss, 1940; Nüske and Fritsche, 1989). However, T3SS-related gene
298 expression inhibition has been reported at 18°C (Arvizu-Gómez et al., 2013), and our results
299 indicate that the strain 1448A is thermo-insensitive in its ability to induce HR. Regarding *P.*
300 *syringae* pv. *actinidiae*, our results confirmed a low-temperature dependency for T3SS efficiency
301 (Puttilli et al., 2022), which is entirely in line with the environmental conditions – in late winter
302 or early spring – under which *P. syringae* pv. *actinidiae* is reported to cause disease or damage in
303 the kiwifruit orchards (Donati et al., 2020; Kim et al., 2017). On the other hand, concerning
304 strains CC0073 and CC0094, isolated from cantaloupe during blight epidemics in southern
305 France in the 90s, the authors have reported that the climatic conditions that favored disease
306 outbreak and development were heavy rainfall associated with a mean minimum temperature
307 below 12-13°C (under which the physiology of cantaloupe comes to a standstill) in 95% of cases,

308 whereas our results demonstrated a major T3SS efficiency at higher temperatures (Mention et
309 al., 2004; Morris and Pitrat, 1998; Riffaud, 2002). Finally, strain DC3000 displays a consistent
310 behavior, exhibiting both unaltered T3SS efficiency and coronatine production in response to
311 temperature, at least within the 18°C to 28°C range (Weingart et al., 2004). Its consistency in
312 response to various environmental parameters, associated with high reproducibility of data
313 related to it, has certainly contributed to making it the model strain it has become. However, this
314 strain was generated in the laboratory as a rifampicin-resistant derivative of the strain DC52,
315 which originated from Guernsey in 1960 (Cuppels, 1986; Xin et al., 2018). Therefore, no
316 conclusive connection could be established between its ecology and its virulence behavior in
317 response to temperature, as this model strain has evolved for many years in laboratories, far
318 from a field context.
319 Our results also provide evidence that growth optima – at least *in vitro* – are not correlated with
320 T3SS efficiency. This contributes to the debate about the question of whether the temperature
321 conditions that favor virulence (specifically T3SS) are identical to those reported as favorable for
322 disease development. Answering this question is challenging due to both supporting and
323 opposing examples when accounting for the various traits characterizing phytopathogenic
324 bacteria that are thermo-sensitive, and each pathogen is characterized by growth and virulence
325 mechanisms that are activated at precise temperatures, generating a complex scenario in which
326 temperature can alter the outcome of the interaction between plant and bacterium by
327 differentially influencing a spectrum of virulence traits (Tribelli and López, 2022). Consequently,
328 it is likely to be very difficult to simplify or generalize the behavior of different strains relative to
329 the influence of temperature on their virulence.

330

331 **Inter-strain variability.**

332 We observed that the behavior of high temperature-preference/dependency is exclusive to
333 strains from phylogroup 2d, whereas the opposite case is specific to strains belonging to
334 phylogroups 1a and 1b. This suggests that temperature responsiveness patterns might vary
335 among strains but remain consistent within the same phylogroup. While the temperature
336 sensitivity feature is widely distributed among the strains, the preference/dependency on low or
337 high temperatures in case of thermosensitivity is conserved within a same phylogroup.
338 Therefore, the preference/dependency on low or high temperatures could be linked to the
339 evolutionary history of pathogens, which may have been shaped by temperature-related
340 selection pressures. Investigating this question would help shed light on the origin of the
341 phenomenon. On the other hand, one important conclusion of our work is the significant
342 variability in behavior among strains, even when closely related at the genomic level (as
343 illustrated with the 3 'CC' strain-quasi-clones). Over the years of research on these issues,
344 examples of such inherent variability in terms of virulence have been largely overlooked, with
345 only a few cases reported in literature, both beyond and within the *P. syringae* species complex
346 (Baron et al., 2001; Hasegawa et al., 2005; Rohde et al., 1998; Weingart et al., 2004). Here, we
347 emphasize the urgent need to study the diversity among strains, since evidence of their inherent
348 variability has been documented. Although investigating model strains has facilitated the
349 understanding and characterization of intricate molecular mechanisms in plant-pathogen
350 interactions, it is now imperative to consider the full spectrum of *P. syringae* species complex

351 diversity (Berge et al., 2014; Gomila et al., 2017), both within and outside of the agronomic
352 context.
353

354 Experimental procedures

355 Bacterial strains, culture conditions and transformation

356 Thirteen *Pseudomonas syringae* strains were selected for this study (Supplementary Table S1;
357 Supplementary information). Wild-type (WT) *P. syringae* strains were grown at 28°C on King's B
358 agar (KB) (King et al., 1954) – supplemented with rifampicin at 50µg/mL for DC3000 and B728a
359 strains. Kanamycin at 50µg/mL was added for the culture of *avrB*-expressing strains. Single
360 colonies of each strain were picked and grown overnight in liquid KB medium – supplemented
361 with rifampicin at 50µg/mL for DC3000 and B728a strains and with kanamycin at 50µg/mL for
362 *avrB*-expressing strains, with agitation at 190 rpm at 28°C.
363 Selected strains were transformed with the pure plasmid carrying *avrB* gene whose sequence
364 was originally isolated from the soybean pathogen *Pseudomonas syringae* pv. *glycinea* (pVB01
365 Km^R; Innes et al., 1993) through electroporation process. Briefly, fresh suspensions of WT strains
366 grown overnight in liquid KB (190 rpm, 28°C) were washed three times and resuspended in 50-
367 100uL of cold 10% glycerol. Pure plasmid (50-250ng) was added to the suspensions which were
368 then transferred into cold 2mm electroporation cuvettes (BioRad, CA, USA) Electroporation was
369 performed with a MicroPulser™ machine (BioRad, CA, USA) set at 1.8-2.5kV. Cells were
370 immediately recovered into fresh nonselective liquid KB medium and incubated at 28°C for 1-2h
371 at 190 rpm. Transformed strains were selected using kanamycin at 50µg/mL (plus rifampicin at
372 50µg/mL for DC3000 and B728a strains) and the presence of the plasmid was confirmed by

373 colony PCR using Promega GoTaq™ DNA polymerase (Fisher Scientific, USA) and specific primers
374 (FOR: ATGGGCTGCGTCTCGTCAAAAAGCA, REV: TTAAAAGCAATCAGAATCTAGCAAG, annealing
375 temperature = 65°C).
376
377 ***avrB* expression control**
378 Relative expression levels of *avrB* in transformed strains were evaluated by real-time PCR. Four
379 mL of fresh suspension of *avrB*-transformed *P. syringae* strains grown overnight in selective
380 medium were centrifuged (5min at 4500g at RT) and total RNA was extracted from pellets using
381 TRIzol substitute (EuroGold TriFast™ Kit, EuroClone, Italy) according to manufacturer
382 instructions. Extraction yield and quality of the transcripts were checked by spectrophotometry
383 (NanoDrop™, Thermo Fisher Scientific, USA). Samples with absorbance ratios A_{260nm}/A_{230nm}
384 and/or A_{260nm} /A_{280nm} outside the range of [2 ± 0.5] were subjected to a lithium chloride
385 treatment to increase their purity (2.5M LiCl, 50mM EDTA, pH 8.0). One to two µg of RNA per
386 sample underwent DNase treatment (TURBO™ DNase, Life Technologies, USA) then the single-
387 stranded complementary DNA synthesis was performed from 0.5-1µg of template RNA using
388 SuperScript™ III Reverse Transcriptase enzyme (Invitrogen, USA) according to manufacturer
389 instructions. Samples get 10-fold diluted and the procedure was performed using Luna®
390 Universal qPCR Master Mix (New England Biolabs, USA). To normalize the expression of the
391 target gene, *rpoD* was chosen as a stable and robust housekeeping gene in *Pseudomonas*
392 (Narusaka et al., 2011; Savli et al., 2003). Amplification was run on a QuantStudio™ 3 real-time
393 PCR system (Applied Biosystems, USA) (primers *avrB* FOR: ATACTCTGCATTCGCCTCCG, REV:
394 TCAACGACTCTGGCAAGGAC; primers *rpoD* FOR: AACTTGCGTCTGGTGATCTC, REV:

395 ATCAAGCCGATGTTGCCTTC). Expression of *avrB* was determined using the $2^{-\Delta\Delta Ct}$ method and
396 normalized against *rpoD*, and fold-change for each strain was established relative to the strain
397 DC3000 *avrB*.
398
399 **Ion-leakage experiments**
400 Hypersensitive response (HR) induction was assessed by quantifying programmed cell death
401 through ion-leakage measurement, as previously published (Imanifard et al., 2018; Jayaraman et
402 al., 2021; Johansson et al., 2015) with slight modifications provided as Supplementary Material.
403
404 **Statistical analysis**
405 For each technical replicate, the conductivity value from the first measure was subtracted to
406 values measured at each successive time points for normalization (Puttilli et al., 2022). For each
407 strain-temperature modality within each replicated experiment, conductivity was calculated as
408 the average of the values of the three technical replicates for each time point, and ion-leakage
409 curves over time were established accordingly. Area under each single conductivity progress
410 curve was calculated (AUCPC), as well as variance and mean AUCPC per modality. Moreover,
411 conductivity values corresponding to 24 hpi as well as the time point for which half of this value
412 was reached for each experiment were calculated via linear interpolation, and this variable
413 $hpi_{50\%}$ was used as a dynamic parameter, indicating how fast a given strain induced HR at a given
414 temperature. Comparison of strains based on this parameter was assessed by variance analysis
415 (Kruskal-Wallis's test) followed by a post-hoc Dunn's test. The same procedure was conducted to

416 compare the three different temperatures regardless of the strain. Data were represented by
417 boxplots.
418 Each single conductivity progress curve constituted from 6 to 9 time points and was considered
419 as one statistical individual (*i.e.*, one iteration) to fit Linear Mixed-effects Models (LMM). Details
420 of the approach are provided as Supplementary Material.
421
422 ***In vitro* HrpZ secretion**
423 Twenty mL of fresh suspension of *avrB*-expressing *P. syringae* strains grown overnight in
424 selective medium were centrifuged (5min at 4500g at room temperature) and pellets were
425 washed three times in 10mL of sterile minimal medium (HIM). OD_{600} was measured with a
426 spectrophotometer (Evolution™, ThermoFisher Scientific, USA) and bacterial cells were
427 resuspended in sterile HIM to 7 x 10^8 CFU/mL (OD_{600nm} = 0.7; final volume = 150mL).
428 Suspensions were divided into three portions of 50mL, each was separately incubated at 18°C,
429 24°C or 28°C with agitation at 190 rpm. After 5 and 24 hours of incubation, 25mL of each
430 bacterial suspension were sampled and OD_{600} was measured again. Cell-free culture supernatant
431 was obtained by centrifugation and filtration, and secreted proteins were precipitated with
432 trichloroacetic acid (TCA) 5% as previously described (Flaugnatti and Journet, 2017; Kobayashi et
433 al., 1997).
434 For immunoblotting, proteins were separated on SDS–polyacrylamide gel electrophoresis and
435 then transferred onto a nitrocellulose blotting membrane (GE HealthCare, USA) using an
436 electrophoretic apparatus. Protein detection was performed using anti-HrpZ (1:5000) (Alfano et
437 al., 1996) and anti-rabbit (1:10000) conjugated with horseradish peroxidase as secondary

438 antibody. To confirm the correct loading ratio among wells, one gel was stained with a
439 Coomassie R-250 staining solution (25% isoprophyl alcohol, 10% acetid acid, 0.05% Coomassie
440 R-250) and destained with 10% acetic acid.
441
442 ***In vitro* growth measurement**
443 Four mL of fresh suspension of *avrB*-expressing *P. syringae* strains grown overnight in selective
444 medium were centrifuged (5min at 4500g at room temperature) and pellets were washed three
445 times in 1mL of fresh liquid KB. Optical density at 600nm was measured by spectrophotometer
446 (Evolution™, ThermoFisher Scientific, USA) and bacterial cells were then resuspended to reach 2
447 x 10^7 CFU/mL (OD_{600nm} = 0.02; final volume = 2mL). Suspensions were aliquoted in a microtiter
448 plate (200µL per well), with 6 technical replicates per strain, and plates were incubated at 18°C,
449 24°C and 28°C. Liquid KB (supplemented or not with the antibiotics) was used as negative
450 control. Absorbance at 600nm was measured every 1.5-2 hours during the first 8 hours of the
451 experiment, and then two or three times between 18 and 24 hpi, obtaining from 6 to 9
452 absorbance measures per well. To eliminate unspecific absorbance signals due to the color of KB
453 medium and the antibiotics, the value from the first measure was subtracted from values
454 measured at each successive time points. Absorbance was then calculated as the average of the
455 values of the six technical replicates for each time point, and bacterial growth curves over time
456 were established accordingly. Each strain-temperature modality was reproduced at least twice,
457 except for T1.
458
459 **Acknowledgments**

460 We thank Pr. Boris A. Vinatzer, Dr. Perrine Portier, and Dr. Marco Scortichini for kindly providing
461 *P. syringae* strains used in this study in addition to our own strains. We also thank Pr. Sheng-Yang
462 He for providing the antibody anti-HrpZ. Special thanks to Pr. Roberto Chignola and Dr. Davide
463 Martinetti for their help in statistical analyzes of ion-leakage data. Finally, we also thank the
464 members of the Biotechnology Department of the University of Verona who provided technical
465 support in conductivity measurements.

466

467 **Data Availability Statement**

468 All data needed to evaluate the conclusions in the paper are present in the paper and/or the
469 Supporting Information. Additional data related to this paper may be requested to the authors.

470

471 **References**

472 Aguilera, S., Alvarez-Morales, A., Murillo, J., Hernández-Flores, J.L., Bravo, J. & De la Torre-
473 Zavala, S. (2017) Temperature-mediated biosynthesis of the phytotoxin phaseolotoxin by
474 *Pseudomonas syringae* pv. *phaseolicola* depends on the autoregulated expression of the
475 *phtABC* genes. *PLOS ONE*, 12, e0178441. https://doi.org/10.1371/journal.pone.0178441.
476 Aguilera, S., López-López, K., Nieto, Y., Garcidueñas-Piña, R., Hernández-Guzmán, G.,
477 Hernández-Flores, J.L., et al. (2007) Functional characterization of the gene cluster from
478 *Pseudomonas syringae* pv. *phaseolicola* NPS3121 involved in synthesis of phaseolotoxin.
479 *Journal of Bacteriology*, 189, 2834. https://doi.org/10.1128/JB.01845-06.
480 Alfano, J.R., Bauer, D.W., Milos, T.M. & Collmer, A. (1996) Analysis of the role of the
481 *Pseudomonas syringae* pv. *syringae* HrpZ harpin in elicitation of the hypersensitive

482 response in tobacco using functionally non-polar *hrpZ* deletion mutations, truncated
483 HrpZ fragments, and *hrmA* mutatio. *Molecular Microbiology*, 19, 715–728.
484 https://doi.org/10.1046/j.1365-2958.1996.415946.x.
485 Arvizu-Gómez, J.L., Hernández-Morales, A., Aguilar, J.R.P. & Álvarez-Morales, A. (2013)
486 Transcriptional profile of *P. syringae* pv. *phaseolicola* NPS3121 at low temperature:
487 physiology of phytopathogenic bacteria. *BMC Microbiology*, 13, 81.
488 https://doi.org/10.1186/1471-2180-13-81.
489 Baltrus, D.A., McCann, H.C. & Guttman, D.S. (2017) Evolution, genomics and epidemiology of
490 *Pseudomonas syringae*. *Molecular Plant Pathology*, 18, 152–168.
491 https://doi.org/10.1111/MPP.12506.
492 Baron, C., Domke, N., Beinhofer, M. & Hapfelmeier, S. (2001) Elevated temperature
493 differentially affects virulence, VirB protein accumulation, and T-pilus formation in
494 different *Agrobacterium tumefaciens* and *Agrobacterium vitis* strains. *Journal of*
495 *Bacteriology*, 183, 6852–6861. https://doi.org/10.1128/JB.183.23.6852-6861.2001.
496 Bender, C.L., Alarcón-Chaidez, F. & Gross, D.C. (1999) *Pseudomonas syringae* phytotoxins: mode
497 of action, regulation, and biosynthesis by peptide and polyketide synthetases.
498 *Microbiology and Molecular Biology Reviews*, 63, 266–292.
499 https://doi.org/10.1128/MMBR.63.2.266-292.1999.
500 Berge, O., Monteil, C.L., Bartoli, C., Chandeysson, C., Guilbaud, C., Sands, D.C., et al. (2014) A
501 user's guide to a data base of the diversity of *Pseudomonas syringae* and its application
502 to classifying strains in this phylogenetic complex. *PLoS ONE*, 9, e105547.
503 https://doi.org/10.1371/journal.pone.0105547.

504 Braun, Y., Smirnova, A.V., Weingart, H., Schenk, A. & Ullrich, M.S. (2009) Coronatine gene
505 expression *in vitro* and *in planta*, and protein accumulation during temperature
506 downshift in *Pseudomonas syringae*. *Sensors*, 9, 4272–4285.
507 https://doi.org/10.3390/s90604272.
508 Büttner, D. & He, S.Y. (2009) Type III protein secretion in plant pathogenic bacteria. *Plant*
509 *Physiology*, 150, 1656–1664. https://doi.org/10.1104/PP.109.139089.
510 Chang, J.H., Urbach, J.M., Law, T.F., Arnold, L.W., Hu, A., Gombar, S., et al. (2005) A high-
511 throughput, near-saturating screen for type III effector genes from *Pseudomonas*
512 *syringae*. *Proceedings of the National Academy of Sciences of the United States of*
513 *America*, 102, 2549–2554. https://doi.org/10.1073/pnas.0409660102.
514 Cheng, C., Gao, X., Feng, B., Sheen, J., Shan, L. & He, P. (2013) Plant immune response to
515 pathogens differs with changing temperatures. *Nature communications*, 4, 2530.
516 https://doi.org/10.1038/ncomms3530.
517 Crabill, E., Joe, A., Block, A., Rooyen, J.M. van & Alfano, J.R. (2010) Plant immunity directly or
518 indirectly restricts the injection of type III effectors by the *Pseudomonas syringae* type III
519 secretion system. *Plant Physiology*, 154, 233–244.
520 https://doi.org/10.1104/pp.110.159723.
521 Cunnac, S., Lindeberg, M. & Collmer, A. (2009) *Pseudomonas syringae* type III secretion system
522 effectors: repertoires in search of functions. *Current Opinion in Microbiology*, 12, 53–60.
523 https://doi.org/10.1016/j.mib.2008.12.003.

524 Cuppels, D.A. (1986) Generation and characterization of Tn5 insertion mutations in
525 *Pseudomonas syringae* pv. *tomato*. *Applied and Environmental Microbiology*, 51, 323–
526 327. https://doi.org/10.1128/aem.51.2.323-327.1986.
527 Czajkowski, R., Kaczyńska, N., Jafra, S., Narajczyk, M. & Lojkowska, E. (2017) Temperature-
528 responsive genetic loci in pectinolytic plant pathogenic *Dickeya solani*. *Plant Pathology*,
529 66, 584–594. https://doi.org/10.1111/PPA.12618.
530 Dillon, M.M., Almeida, R.N.D., Laflamme, B., Martel, A., Weir, B.S., Desveaux, D., et al. (2019)
531 Molecular evolution of *Pseudomonas syringae* type III secreted effector proteins.
532 *Frontiers in plant science*, 10, 418. https://doi.org/10.3389/fpls.2019.00418.
533 Donati, I., Cellini, A., Sangiorgio, D., Vanneste, J.L., Scortichini, M., Balestra, G.M., et al. (2020)
534 *Pseudomonas syringae* pv. *actinidiae*: ecology, infection dynamics and disease
535 epidemiology. *Microbial Ecology*, 80, 81–102. https://doi.org/10.1007/s00248-019-
536 01459-8.
537 Flaugnatti, N. & Journet, L. (2017) Identification of effectors: precipitation of supernatant
538 material. Bacterial Protein Secretion Systems. pp. 459–464.
539 Galán, J.E. & Collmer, A. (1999) Type III secretion machines: bacterial devices for protein
540 delivery into host cells. *Science*, 284, 1322–1328.
541 https://doi.org/10.1126/science.284.5418.1322.
542 Gomila, M., Busquets, A., Mulet, M., García-Valdés, E. & Lalucat, J. (2017) Clarification of
543 taxonomic status within the *Pseudomonas syringae* species group based on a
544 phylogenomic analysis. *Frontiers in Microbiology*, 8, 320397.
545 https://doi.org/10.3389/fmicb.2017.02422.

546 Goss, R.W. (1940) The relation of temperature to common and halo blight of Beans.
547 *Phytopathology*, 30. https://doi.org/10.5555/19401101012.
548 Guo, M., Tian, F., Wamboldt, Y. & Alfano, J.R. (2009) The majority of the type III effector
549 inventory of *Pseudomonas syringae* pv. *tomato* DC3000 can suppress plant immunity.
550 *Molecular Plant-Microbe Interactions*, 22, 1069–1080. https://doi.org/10.1094/MPMI-
551 22-9-1069.
552 Guttman, D.S., Vinatzer, B.A., Sarkar, S.F., Ranall, M.V., Kettler, G. & Greenberg, J.T. (2002) A
553 functional screen for the type III (Hrp) secretome of the plant pathogen *Pseudomonas*
554 *syringae*. *Science*, 295, 1722–1726. https://doi.org/10.1126/science.295.5560.1722.
555 Hasegawa, H., Chatterjee, A., Cui, Y. & Chatterjee, A.K. (2005) Elevated temperature enhances
556 virulence of *Erwinia carotovora* subsp. *carotovora* strain EC153 to plants and stimulates
557 production of the quorum sensing signal, N -acyl homoserine lactone, and extracellular
558 proteins. *Applied and Environmental Microbiology*, 71, 4655–4663.
559 https://doi.org/10.1128/AEM.71.8.4655-4663.2005.
560 Hockett, K.L., Burch, A.Y. & Lindow, S.E. (2013) Thermo-regulation of genes mediating motility
561 and plant interactions in *Pseudomonas syringae*. *PLoS ONE*, 8, e59850.
562 https://doi.org/10.1371/journal.pone.0059850.
563 Hua, J. (2014) Temperature and plant immunity. Temperature and Plant Development. Wiley,
564 pp. 163–180.
565 Hueck, C.J. (1998) Type III protein secretion systems in bacterial pathogens of animals and
566 plants. *Microbiology and molecular biology reviews: MMBR*, 62, 379–433.
567 https://doi.org/10.1128/mmbr.62.2.379-433.1998.

568 Huot, B., Castroverde, C.D.M., Velásquez, A.C., Hubbard, E., Pulman, J.A., Yao, J., et al. (2017)
569 Dual impact of elevated temperature on plant defence and bacterial virulence in
570 *Arabidopsis*. *Nature Communications*, 8, 1808. https://doi.org/10.1038/s41467-017-
571 01674-2.
572 Imanifard, Z., Vandelle, E. & Bellin, D. (2018) Measurement of hypersensitive cell death
573 triggered by avirulent bacterial pathogens in *Arabidopsis*. *Methods in Molecular Biology*,
574 1743, 39–50. https://doi.org/10.1007/978-1-4939-7668-3_4.
575 Innes, R.W., Bisgrove, S.R., Smith, N.M., Bent, A.F., Staskawicz, B.J. & Liu, Y. (1993) Identification
576 of a disease resistance locus in *Arabidopsis* that is functionally homologous to the *RPG1*
577 locus of soybean. *The Plant Journal*, 4, 813–820. https://doi.org/10.1046/j.1365-
578 313X.1993.04050813.x.
579 Jamir, Y., Guo, M., Oh, H., Petnicki-Ocwieja, T., Chen, S., Tang, X., et al. (2004) Identification of
580 *Pseudomonas syringae* type III effectors that can suppress programmed cell death in
581 plants and yeast. *The Plant Journal*, 37, 554–565. https://doi.org/10.1046/j.1365-
582 313X.2003.01982.x.
583 Jayaraman, J., Chatterjee, A., Hunter, S., Chen, R., Stroud, E.A., Saei, H., et al. (2021) Rapid
584 methodologies for assessing *Pseudomonas syringae* pv. *actinidiae* colonization and
585 effector-mediated hypersensitive response in kiwifruit. *Molecular plant-microbe*
586 *interactions: MPMI*, 34, 880–890. https://doi.org/10.1094/MPMI-02-21-0043-R.
587 Jin, Q. & He, S.-Y. (2001) Role of the Hrp pilus in type III protein secretion in *Pseudomonas*
588 *syringae*. *Science*, 294, 2556–2558. https://doi.org/10.1126/science.1066397.

589 Johansson, O.N., Nilsson, A.K., Gustavsson, M.B., Backhaus, T., Andersson, M.X. & Ellerström, M.
590 (2015) A quick and robust method for quantification of the hypersensitive response in
591 plants. *PeerJ*, 3, e1469. https://doi.org/10.7717/peerj.1469.
592 Kim, G.H., Jung, J.S. & Koh, Y.J. (2017) Occurrence and epidemics of bacterial canker of kiwifruit
593 in Korea. *The plant pathology journal*, 33, 351–361.
594 https://doi.org/10.5423/PPJ.RW.01.2017.0021.
595 King, E.O., Ward, M.K. & Raney, D.E. (1954) Two simple media for the demonstration of
596 pyocyanin and fluorescin. *The journal of laboratory and clinical medicine*, 44, 301–307.
597 Klinkert, B. & Narberhaus, F. (2009) Microbial thermosensors. *Cellular and molecular life*
598 *sciences: CMLS*, 66, 2661–2676. https://doi.org/10.1007/s00018-009-0041-3.
599 Kobayashi, T., Kishigami, S., Sone, M., Inokuchi, H., Mogi, T. & Ito, K. (1997) Respiratory chain is
600 required to maintain oxidized states of the DsbA-DsbB disulfide bond formation system
601 in aerobically growing *Escherichia coli* cells. *Proceedings of the National Academy of*
602 *Sciences of the United States of America*, 94, 11857–11862.
603 https://doi.org/10.1073/pnas.94.22.11857.
604 Krishna, P.S., Woodcock, S.D., Pfeilmeier, S., Bornemann, S., Zipfel, C. & Malone, J.G. (2022)
605 *Pseudomonas syringae* addresses distinct environmental challenges during plant
606 infection through the coordinated deployment of polysaccharides. *Journal of*
607 *Experimental Botany*, 73, 2206–2221. https://doi.org/10.1093/jxb/erab550.
608 Kubori, T., Shinzawa, N., Kanuka, H. & Nagai, H. (2010) *Legionella* metaeffector exploits host
609 proteasome to temporally regulate cognate effector. *PLoS Pathogens*, 6, e1001216.
610 https://doi.org/10.1371/journal.ppat.1001216.

611 Künstler, A., Bacsó, R., Gullner, G., Hafez, Y.M. & Király, L. (2016) Staying alive – is cell death
612 dispensable for plant disease resistance during the hypersensitive response?
613 *Physiological and molecular plant pathology*, 93, 75–84.
614 https://doi.org/10.1016/j.pmpp.2016.01.003.
615 Laflamme, B., Dillon, M.M., Martel, A., Almeida, R.N.D., Desveaux, D. & Guttman, D.S. (2020)
616 The pan-genome effector-triggered immunity landscape of a host-pathogen interaction.
617 *Science*, 367, 763–768. https://doi.org/10.1126/science.aax4079.
618 Lamichhane, J.R., Messéan, A. & Morris, C.E. (2015) Insights into epidemiology and control of
619 diseases of annual plants caused by the *Pseudomonas syringae* species complex. *Journal*
620 *of General Plant Pathology*, 81, 331–350. https://doi.org/10.1007/s10327-015-0605-z.
621 Lamichhane, J.R., Varvaro, L., Parisi, L., Audergon, J.-M. & Morris, C.E. (2014) Disease and frost
622 damage of woody plants caused by *Pseudomonas syringae*. Advances in Agronomy. pp.
623 235–295.
624 Lee, C.A. (1997) Type III secretion systems: machines to deliver bacterial proteins into
625 eukaryotic cells? *Trends in microbiology*, 5, 148–156. https://doi.org/10.1016/S0966-
626 842X(97)01029-9.
627 Li, C.M. (2002) The Hrp pilus of *Pseudomonas syringae* elongates from its tip and acts as a
628 conduit for translocation of the effector protein HrpZ. *The EMBO Journal*, 21, 1909–
629 1915. https://doi.org/10.1093/emboj/21.8.1909.
630 Li, H., Schenk, A., Srivastava, A., Zhurina, D. & Ullrich, M.S. (2006) Thermo-responsive expression
631 and differential secretion of the extracellular enzyme levansucrase in the plant

632 pathogenic bacterium *Pseudomonas syringae* pv. *glycinea*. *FEMS Microbiology Letters*,
633 265, 178–185. https://doi.org/10.1111/J.1574-6968.2006.00486.X.
634 Lindeberg, M., Cunnac, S. & Collmer, A. (2012) *Pseudomonas syringae* type III effector
635 repertoires: last words in endless arguments. *Trends in Microbiology*, 20, 199–208.
636 https://doi.org/10.1016/j.tim.2012.01.003.
637 Mackey, D., Holt, B.F., Wiig, A. & Dangl, J.L. (2002) RIN4 interacts with *Pseudomonas syringae*
638 type III effector molecules and is required for RPM1-mediated resistance in *Arabidopsis*.
639 *Cell*, 108, 743–754. https://doi.org/10.1016/S0092-8674(02)00661-X.
640 Martel, A., Laflamme, B., Breit-McNally, C., Wang, P., Lonjon, F., Desveaux, D., et al. (2022)
641 Metaeffector interactions modulate the type III effector-triggered immunity load of
642 *Pseudomonas syringae*. *PLoS Pathogens*, 18, e1010541.
643 https://doi.org/10.1371/journal.ppat.1010541.
644 Menna, A., Nguyen, D., Guttman, D.S. & Desveaux, D. (2015) Elevated temperature differentially
645 influences effector-triggered immunity outputs in *Arabidopsis*. *Frontiers in Plant Science*,
646 6, 1–7. https://doi.org/10.3389/fpls.2015.00995.
647 Mention, P., Lavigne, D., Leix-Henry, F., Bouchu, S., Morris, C.E., Prior, P., et al. (2004) Bactériose
648 du melon: acquis et perspectives. *PHM Revue Horticole*, 22–26.
649 Morris, C.E., Lamichhane, J.R., Nikolić, I., Stanković, S. & Moury, B. (2019) The overlapping
650 continuum of host range among strains in the *Pseudomonas syringae* complex.
651 *Phytopathology Research*, 1, 4. https://doi.org/10.1186/s42483-018-0010-6.
652 Morris, C.E. & Pitrat, M. (1998) La bactériose du melon : connaissances acquises et travaux en
653 cours. *PHM Revue Horticole*, 44–47.

654 Mudgett, M.B. (2005) New insights to the function of phytopathogenic bacterial type III
655 effectors in plants. *Annual review of plant biology*, 56, 509–531.
656 https://doi.org/10.1146/annurev.arplant.56.032604.144218.
657 Mudgett, M.B. & Staskawicz, B.J. (1998) Protein signaling via type III secretion pathways in
658 phytopathogenic bacteria. *Current Opinion in Microbiology*, 1, 109–115.
659 https://doi.org/10.1016/S1369-5274(98)80150-1.
660 Narusaka, M., Shiraishi, T., Iwabuchi, M. & Narusaka, Y. (2011) *rpoD* gene expression as an
661 indicator of bacterial pathogens in host plants. *Journal of general plant pathology: JGPP*,
662 77, 75–80. https://doi.org/10.1007/s10327-011-0298-x.
663 Ngou, B.P.M., Ahn, H.-K., Ding, P. & Jones, J.D.G. (2021) Mutual potentiation of plant immunity
664 by cell-surface and intracellular receptors. *Nature*, 592, 110–115.
665 https://doi.org/10.1038/s41586-021-03315-7.
666 Nüske, J. & Fritsche, W. (1989) Phaseolotoxin production by *Pseudomonas syringae* pv.
667 *phaseolicola*: the influence of temperature. *Journal of Basic Microbiology*, 29, 441–447.
668 https://doi.org/10.1002/JOBM.3620290713.
669 Palmer, D.A. & Bender, C.L. (1993) Effects of environmental and nutritional factors on
670 production of the polyketide phytotoxin coronatine by *Pseudomonas syringae* pv.
671 *glycinea*. *Applied and Environmental Microbiology*, 59, 1619–1626.
672 https://doi.org/10.1128/aem.59.5.1619-1626.1993.
673 Peñaloza-Vázquez, A., Kidambi, S.P., Chakrabarty, A.M. & Bender, C.L. (1997) Characterization of
674 the alginate biosynthetic gene cluster in *Pseudomonas syringae* pv. *syringae*. *Journal of*
675 *Bacteriology*, 179, 4464–4472. https://doi.org/10.1128/jb.179.14.4464-4472.1997.

676 Puttilli, M.R., Danzi, D., Correia, C., Brandi, J., Cecconi, D., Manfredi, M., et al. (2022) Plant
677 signals anticipate the induction of the type III secretion system in *Pseudomonas syringae*
678 pv. *actinidiae*, facilitating efficient temperature-dependent effector translocation.
679 *Microbiology Spectrum*, 10. https://doi.org/10.1128/spectrum.02073-22.
680 Riffaud, C. (2002) *La bactériose du melon : écologie et stratégies de lutte contre Pseudomonas*
681 *syringae pv.aptata*. Université Claude Bernard Lyon I.
682 Rohde, B.H., Pohlack, B. & Ullrich, M.S. (1998) Occurrence of thermoregulation of genes
683 involved in coronatine biosynthesis among various *Pseudomonas syringae* strains.
684 *Journal of Basic Microbiology*, 38, 41–50. https://doi.org/10.1002/(SICI)1521-
685 4028(199803)38:1<41::AID-JOBM41>3.0.CO;2-6.
686 Roine, E., Wei, W., Yuan, J., Nurmiaho-Lassila, E.L., Kalkkinen, N., Romantschuk, M., et al. (1997)
687 Hrp pilus: an *hrp*-dependent bacterial surface appendage produced by *Pseudomonas*
688 *syringae* pv. *tomato* DC3000. *Proceedings of the National Academy of Sciences of the*
689 *United States of America*, 94, 3459–3464. https://doi.org/10.1073/pnas.94.7.3459.
690 Savli, H., Karadenizli, A., Kolayli, F., Gundes, S., Ozbek, U. & Vahaboglu, H. (2003) Expression
691 stability of six housekeeping genes: a proposal for resistance gene quantification studies
692 of *Pseudomonas aeruginosa* by real-time quantitative RT-PCR. *Journal of medical*
693 *microbiology*, 52, 403–408. https://doi.org/10.1099/jmm.0.05132-0.
694 Scalschi, L., Fernández-Crespo, E., Pitarch-Marin, M., Llorens, E., González-Hernández, A.I.,
695 Camañes, G., et al. (2022) Response of tomato-*Pseudomonas* pathosystem to mild heat
696 stress. *Horticulturae*, 8, 174. https://doi.org/10.3390/horticulturae8020174.

697 Smirnova, A., Li, H., Weingart, H., Aufhammer, S., Burse, A., Finis, K., et al. (2001)
698 Thermoregulated expression of virulence factors in plant-associated bacteria. *Archives of*
699 *microbiology*, 176, 393–399. https://doi.org/10.1007/s002030100344.
700 Stevens, R.B. (1960) Plant Pathology, an Advanced Treatise, Vol. 3. Horsfall, J.G. and Dimond,
701 A.E. (Eds.). Academic Press, NY.
702 Tribelli, P.M. & López, N.I. (2022) Insights into the temperature responses of *Pseudomonas*
703 species in beneficial and pathogenic host interactions.
704 Ullrich, M.S., Schergaut, M., Boch, J. & Ullrich, B. (2000) Temperature-responsive genetic loci in
705 the plant pathogen *Pseudomonas syringae* pv. *glycinea*. *Microbiology*, 146, 2457–2468.
706 https://doi.org/10.1099/00221287-146-10-2457.
707 Van Dijk, K., Fouts, D.E., Rehm, A.H., Hill, A.R., Collmer, A. & Alfano, J.R. (1999) The Avr (effector)
708 proteins HrmA (HopPsyA) and AvrPto are secreted in culture from *Pseudomonas*
709 *syringae* pathovars via the Hrp (type III) protein secretion system in a temperature- and
710 pH-sensitive manner. *Journal of Bacteriology*, 181, 4790–4797.
711 https://doi.org/10.1128/jb.181.16.4790-4797.1999.
712 Velásquez, A.C., Castroverde, C.D.M. & He, S.Y. (2018) Plant–Pathogen warfare under changing
713 climate conditions.
714 Wang, Y., Bao, Z., Zhu, Y. & Hua, J. (2009) Analysis of temperature modulation of plant defense
715 against biotrophic microbes. *Molecular Plant-Microbe Interactions*, 22, 498–506.
716 https://doi.org/10.1094/MPMI-22-5-0498.
717 Wei, M., KeisukeTakeshima, Yokoyama, T., Minamisawa, K., Mitsui, H., Itakura, M., et al. (2010)
718 Temperature-dependent expression of type III secretion system genes and its regulation

719 in *Bradyrhizobium japonicum*. *Molecular Plant-Microbe Interactions*, 23, 628–637.
720 https://doi.org/10.1094/MPMI-23-5-0628.
721 Wei, M., Yokoyama, T., Minamisawa, K., Mitsui, H., Itakura, M., Kaneko, T., et al. (2008) Soybean
722 seed extracts preferentially express genomic loci of *Bradyrhizobium japonicum* in the
723 initial interaction with soybean, *Glycine max* (L.) Merr. *DNA Research*, 15, 201–214.
724 https://doi.org/10.1093/dnares/dsn012.
725 Weingart, H., Stubner, S., Schenk, A. & Ullrich, M.S. (2004) Impact of temperature on *in planta*
726 expression of genes involved in synthesis of the *Pseudomonas syringae* phytotoxin
727 coronatine. *Molecular Plant-Microbe Interactions*, 17, 1095–1102.
728 https://doi.org/10.1094/MPMI.2004.17.10.1095.
729 Xin, X.-F., Kvitko, B. & He, S.Y. (2018) *Pseudomonas syringae*: what it takes to be a pathogen.
730 *Nature Reviews Microbiology*, 16, 316–328. https://doi.org/10.1038/nrmicro.2018.17.
731 Xin, X.-F., Nomura, K., Aung, K., Velásquez, A.C., Yao, J., Boutrot, F., et al. (2016) Bacteria
732 establish an aqueous living space in plants crucial for virulence. *Nature*, 539, 524–529.
733 https://doi.org/10.1038/nature20166.
734

735 ## Supplementary figure legends

736 **Figure S1. Variance of the mean area under conductivity progress curve (AUCPC) values**
737 **obtained for each 39 modalities *avrB*-expressing strain x temperature.** Number of replicated
738 experiments for each strain varied from 3 up to 27. Linear regression trend curve was fitted to
739 the data, with $y=323.89x - 150932$ and $R^2=0.8588$, showing a positive correlation between mean
740 AUCPC and their variance (Spearman's coefficient = 0.91; $p < 0.05$).

741

742 **Figure S2. avrB expression among the mutant strains.** RNA was extracted from bacterial
743 suspensions grown overnight at 28°C in liquid KB medium supplemented with kanamycin
744 (50µg/mL) and rifampicin (50µg/mL, for DC3000 *avrB* and B728a *avrB* only). Real-time PCR was
745 performed using *rpoD* as the housekeeping gene. Expression levels were established using the
746 2–ΔΔCt method using DC3000 *avrB* as a reference (fold change = 1). Error bars represent
747 standard error. Data represent the mean of three independent biological replicates, each
748 repeated at least twice.

749

750 **Figure S3. *In-vitro* growth curves for DC3000 avrB (a), USA007 avrB (b) and CC0094 avrB (c).**
751 Bacterial growth was measured for 24 hours at 18°C (blue), 24°C (pink) and 28°C (red). Overnight
752 grown bacteria were resuspended in liquid KB medium supplemented with kanamycin
753 (50µg/mL) and rifampicin (50µg/mL, for DC3000 *avrB* only) at an initial load of 107 CFU/mL
754 (optical density measured at 600nm = 0.01). Data represent one single representative biological
755 replicate with all strains and temperature conditions evaluated simultaneously with six technical
756 replicates each. Error bars represent standard error.

757

758 **Figure S4. Electrolyte leakage curves over time obtained post-infiltration for CRA-FRU 8.43 in**
759 ***Actinidia arguta* (a) and CC0094 *in A. thaliana* Col-0 (b).** Infiltrated leaf disks were incubated at
760 18°C (blue) and 28°C (red). Conductivity following infiltration of the mock treatment (10mM
761 $MgCl_2$) and incubation at 18°C is represented by the black dotted line. Data represent one single

762 representative biological replicate with all strains and temperature conditions evaluated
763 simultaneously with three technical replicates each. Error bars represent standard error.
764

765 ## Figure legends

766 **Figure 1. Electrolyte leakage curves obtained post-infiltration for strain M6 *avrB* at 18°C (a),**
767 **USA007 *avrB* at 18°C (b), LAB0041 *avrB* at 24°C (c) and CC1498 *avrB* at 28°C (d).** Each curve
768 represents the mean increase in conductivity measured over time for one independent
769 biological replicate performed with three technical replicates each. Error bars represent
770 standard error. For each curve, the area under the conductivity progress curve (AUCPC) was also
771 calculated, as well as the ratio between the highest and the smallest AUCPC for each strain-
772 temperature couple.
773

774 **Figure 2. Mean area under conductivity progress curve (AUCPC) calculations for all the**
775 **replicated experiments (3 ≤ n ≤ 27) of each *avrB*-expressing strain at 18°C (a), 24°C (b) and 28°C**
776 **(c).** Error bars represent standard error.
777

778 **Figure 3. HrpZ secretion profiles across a range of temperature.** Strains expressing *avrB* were
779 incubated in *hrp*-inducing medium (HIM) at 18°C, 24°C or 28°C for 5 hours. Cell-free culture
780 supernatant was obtained by centrifugation and filtration. Proteins of bacterial culture
781 supernatant were then precipitated with trichloroacetic acid (TCA) and analyzed by Western blot
782 using an anti-HrpZ antibody. The expected molecular weight is *ca.* 40kDa. A mix of samples
783 proven to contain HrpZ in previous replicates was used as the positive control (C+) at two

784 different concentrations (1X and 2X). Samples were run in different gels that were transferred
785 onto membranes whose pictures were cropped and merged into a single figure.
786
787 **Figure 4. Electrolyte leakage curves over time obtained post-infiltration for CC0073 *avrB* (a),**
788 **CC0094 *avrB* (b) and CC1498 *avrB* (c).** Infiltrated leaf disks were incubated at 18°C (blue), 24°C
789 (pink) and 28°C (red). Conductivity following infiltration of the mock treatment (10mM $MgCl_2$)
790 and incubation at 24°C is represented by the black dotted line. Data represent one single
791 representative biological replicate with all strains and temperature conditions evaluated
792 simultaneously with three technical replicates each. Error bars represent standard error.
793
794 **Figure 5**. **Estimation of velocity of HR induction.** The proxy for velocity was calculated as the
795 time point when half of conductivity increase is reached for each *avrB*-expressing strain inducing
796 HR at least at one temperature condition. (a) Strains are sorted by phylogroup from left to right,
797 PG1a (purple), PG1b (green), PG2d (yellow), PG3a (red). Boxes were calculated from 5 up to 73
798 replicated experiments per strain (single dots). Boxes associated with different letters represent
799 significantly different means ($p < 0.05$, according to a Kruskal-Wallis's test followed by post-hoc
800 Dunn's test). (b) Boxes were calculated from 70 to 97 replicated experiments per temperature
801 (single dots). Boxes associated with different letters represent significantly different means ($p <$
802 0.05, according to a Kruskal-Wallis's test followed by post-hoc Dunn's test).

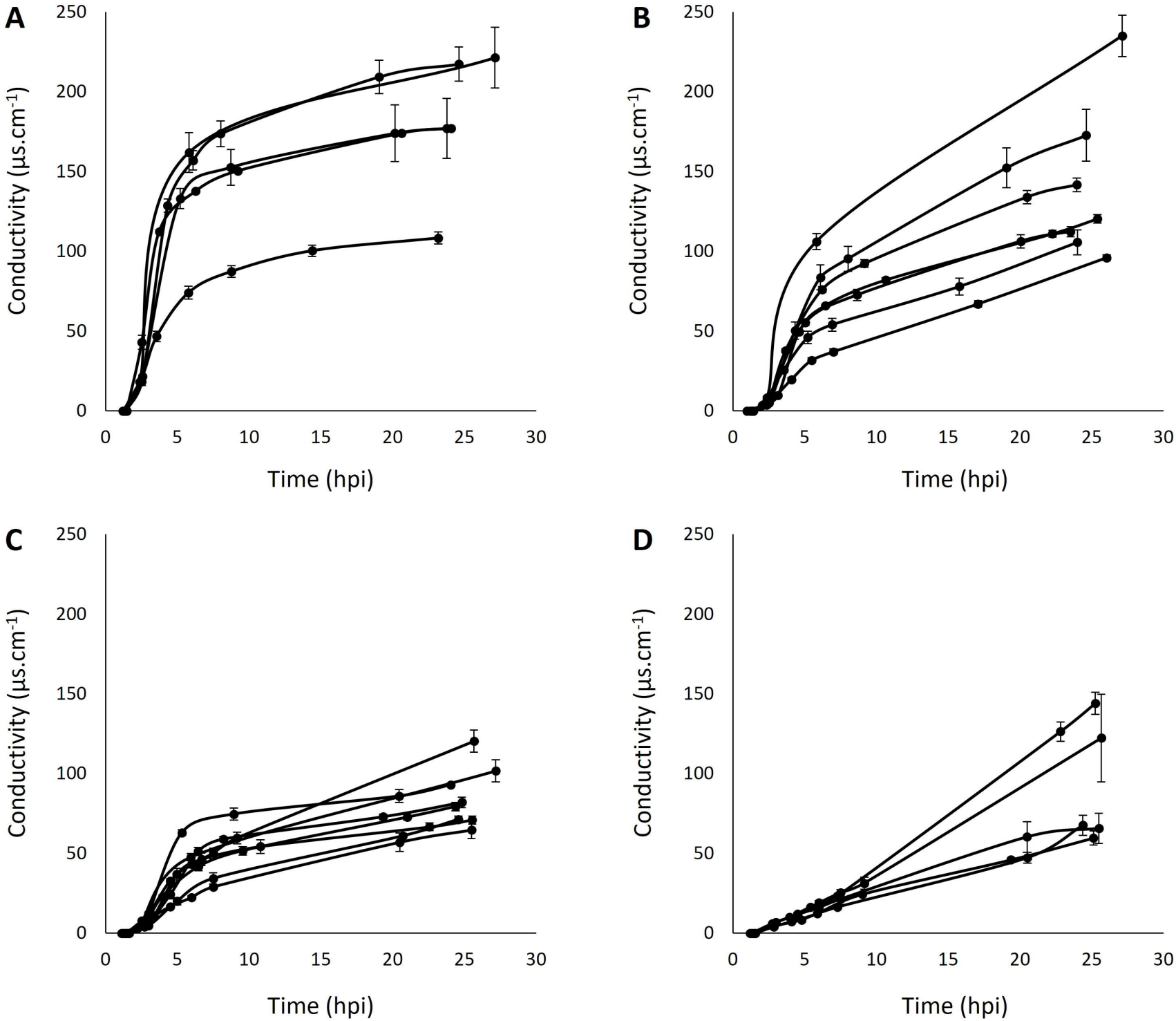
A
B
C
D
Conductivity (µs.cm-1)
Time (hpi)
0
50
100
150
200
250
0
5
10
15
20
25
30

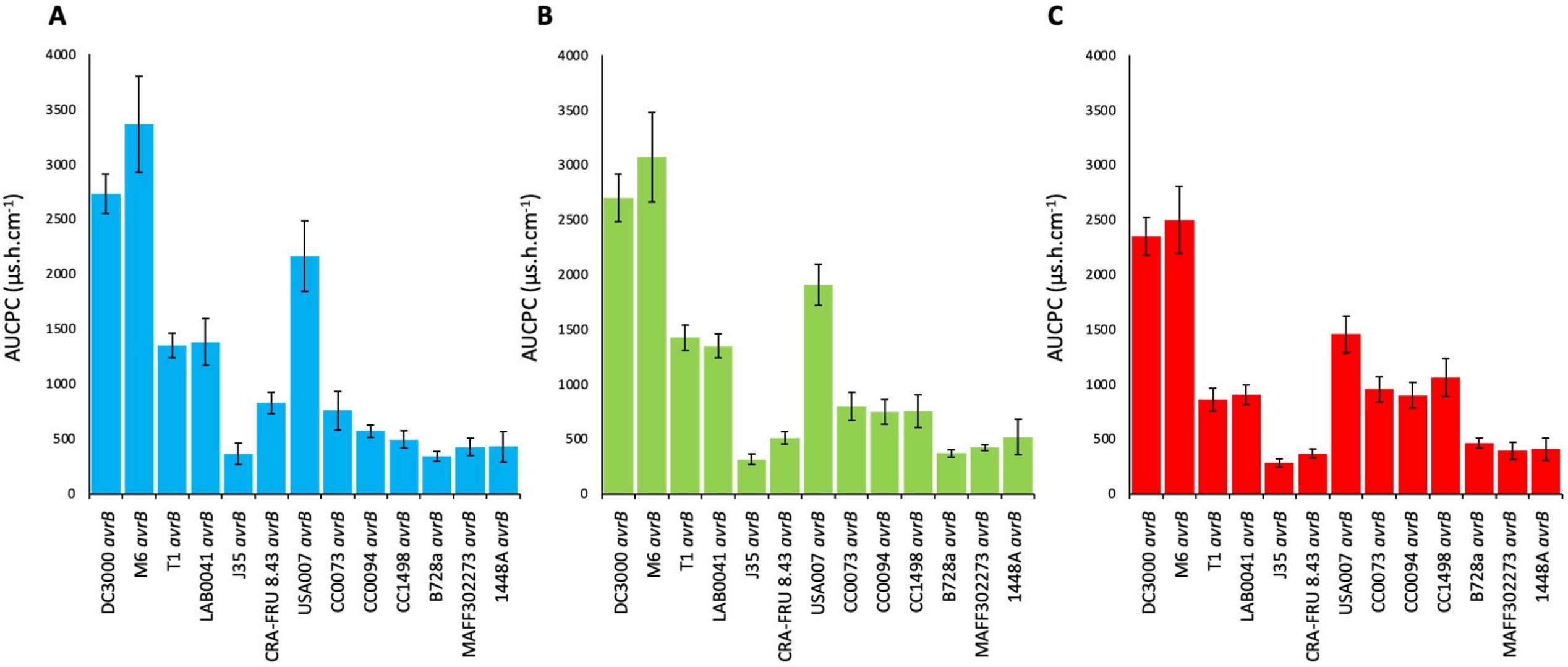
A
B
C
AUCPC (µs.h.cm-1)
4000
3500
3000
2500
2000
1500
1000
500
0
DC3000 avrB
M6 avrB
T1 avrB
LAB0041 avrB
J35 avrB
CRA-FRU 8.43 avrB
USA007 avrB
CC0073 avrB
CC0094 avrB
CC1498 avrB
B728a avrB
MAFF302273 avrB
1448A avrB

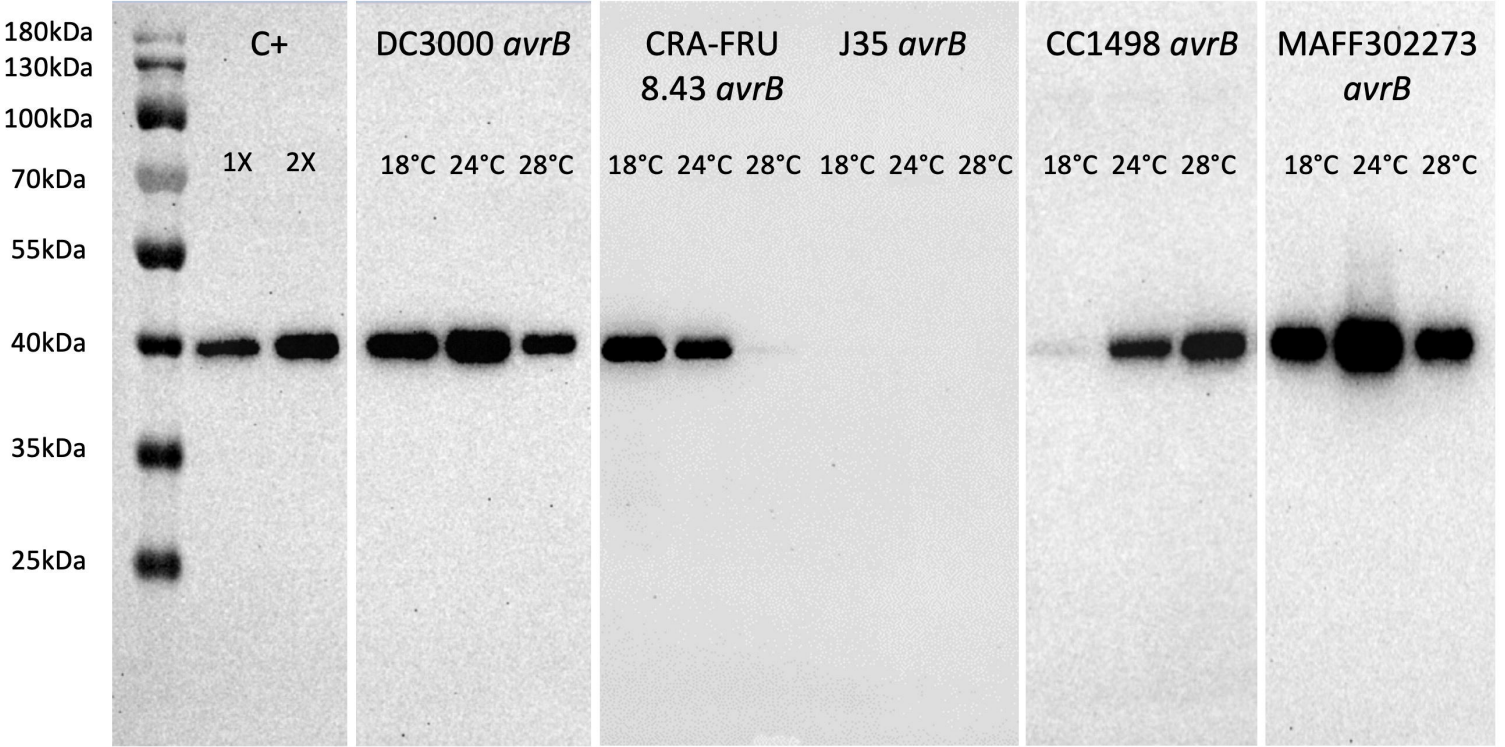
180kDa
130kDa
100kDa
70kDa
55kDa
40kDa
35kDa
25kDa
C+
1X
2X
DC3000 avrB
18°C 24°C 28°C
CRA-FRU 8.43 avrB
18°C 24°C 28°C
J35 avrB
18°C 24°C 28°C
CC1498 avrB
18°C 24°C 28°C
MAFF302273 avrB
18°C 24°C 28°C

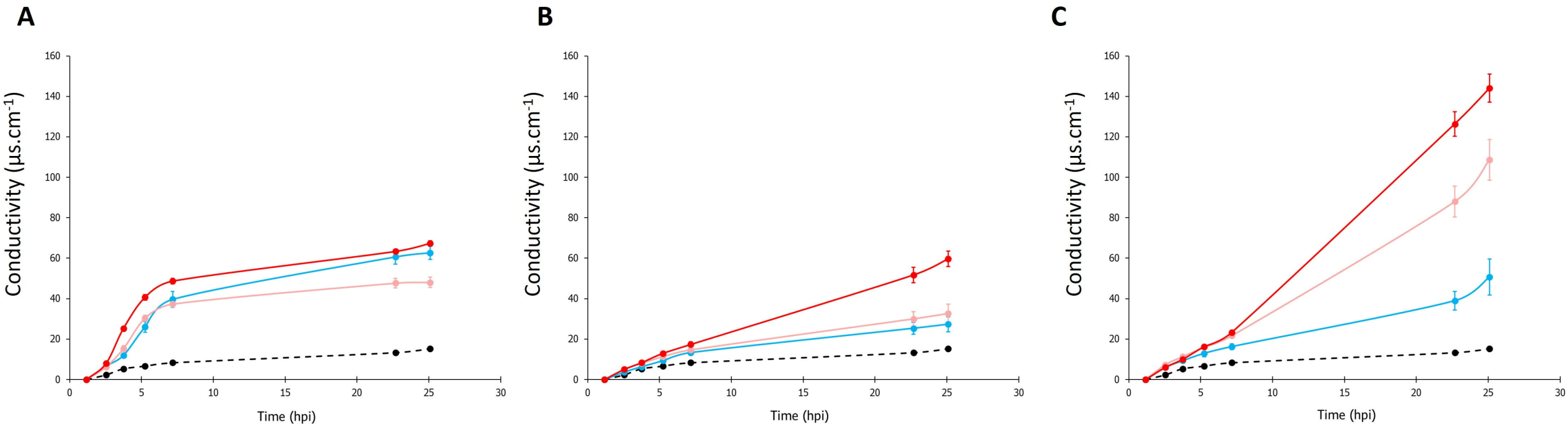
A
B
C
Conductivity (µs.cm-1)
Time (hpi)
0
20
40
60
80
100
120
140
160
0
5
10
15
20
25
30

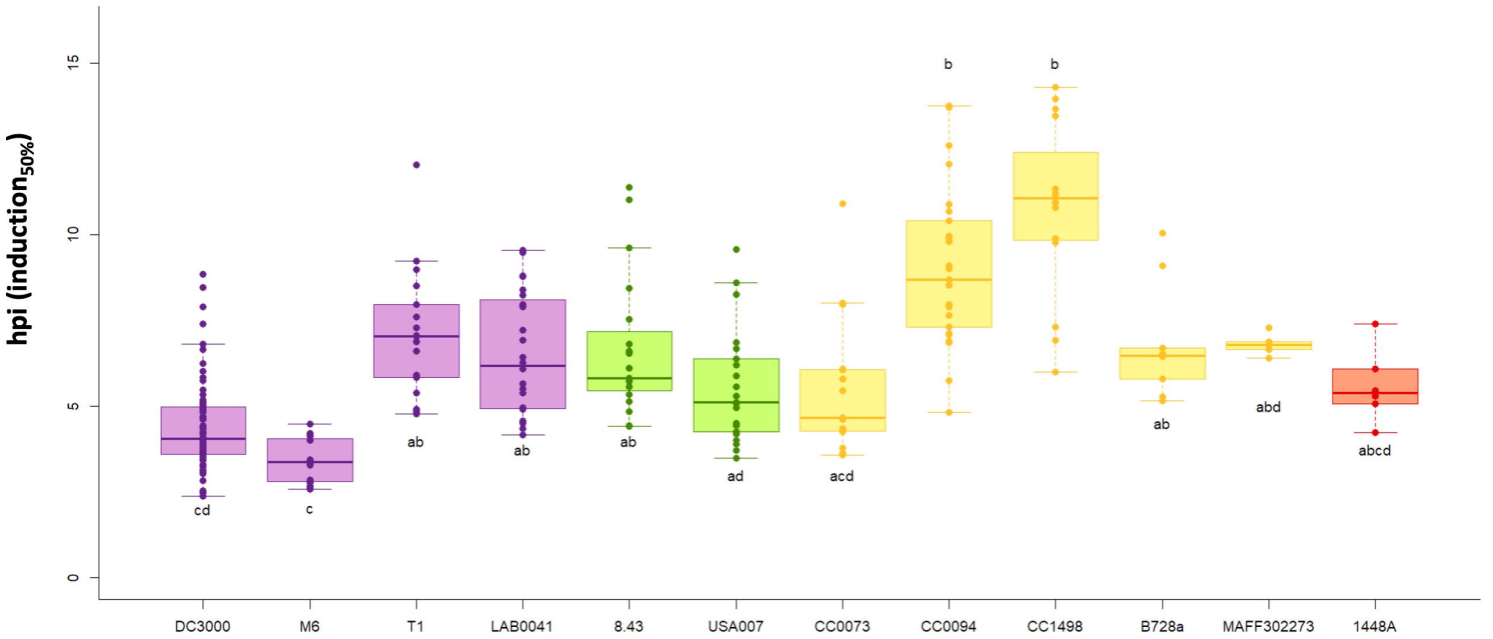
A
hpi (induction50%)
0
5
10
15
cd
c
ab
ab
ab
ad
acd
b
b
ab
abd
abcd
DC3000
M6
T1
LAB0041
8.43
USA007
CC0073
CC0094
CC1498
B728a
MAFF302273
1448A

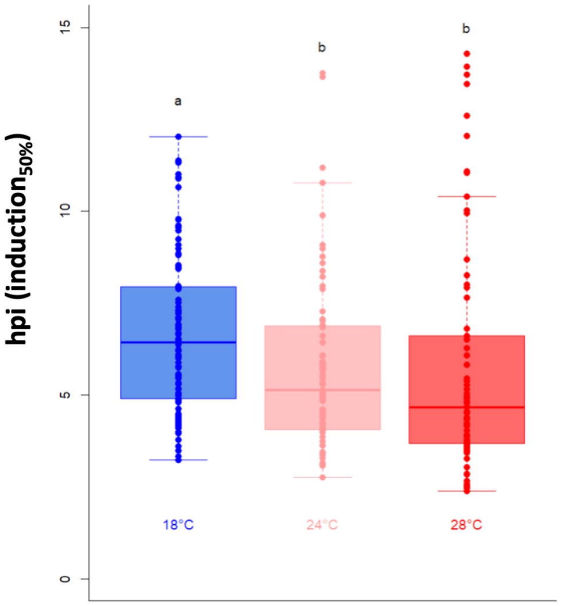
B
hpi (induction50%)
0
5
10
15
a
b
b
18°C
24°C
28°C

Table 1. Statistics associated with linear mixed-effects models fitted to ion leakage experiment results.

PHYLOGROUP	STRAIN	INDUCER AT A GIVEN TEMPERATURE						TEMPERATURE	
		18°C		24°C		28°C			
		Estimate	*p-value*	*Estimate*	*p-value*	*Estimate*	*p-value*	*p-value*	*Estimate*
1a	DC3000	69.97	**2.00E-16**	73.12	**1.25E-15**	65.27	**8.46E-15**	8.02E-01	-0.19
	M6	95.14	**2.00E-16**	89.06	**5.35E-16**	73.05	**1.59E-14**	1.95E-01	-2.07
	T1	28.98	**2.00E-16**	29.07	**2.00E-16**	13.45	**2.81E-08**	**1.42E-02**	**-1.26**
	LAB0041	31.36	**4.24E-11**	29.56	**2.00E-16**	16.83	**2.83E-09**	5.17E-02	-1.22
1b	J35	3.35	5.43E-02	0.18	9.19E-01	-1.27	4.46E-01	NA	
	CRA-FRU 8.43	14.09	**4.69E-11**	4.97	**4.33E-04**	0.97	4.45E-01	**3.80E-03**	**-1.28**
	USA007	52.24	**2.00E-16**	46.69	**8.58E-16**	34.15	**2.26E-12**	**3.35E-02**	**-1.70**
2d	CC0073	15.22	**5.97E-07**	15.28	**7.62E-07**	19.77	**3.42E-09**	3.55E-01	0.63
	CC0094	6.86	**6.44E-08**	9.72	**2.61E-06**	14.49	**8.91E-08**	**9.76E-04**	**0.97**
	CC1498	7.89	**4.96E-06**	12.69	**2.24E-05**	19.96	**1.52E-08**	**2.58E-02**	**1.36**
	B728a	3.12	**2.08E-02**	2.22	1.61E-01	4.75	**8.07E-03**	**4.27E-02**	**0.37**
	MAFF302273	3.17	**1.73E-02**	2.88	9.68E-02	1.78	3.77E-01	NA	
3a	1448A	5.14	**1.07E-02**	6.73	**9.73E-03**	2.46	2.41E-01	6.41E-01	0.53

The effect of strains was calculated for each mutant bacterium at each temperature by comparing with the results obtained for the mock treatment (10mM $MgCl_2$). Significant values of the estimate parameter ($p < 0.05$, in bold) are associated with HR inducing conditions. The temperature effect was evaluated for each *avrB*-expressing strain, inducing HR at least at two temperatures (non-inducer strains are highlighted in grey), comparing the electrolyte leakage curves obtained at these different temperatures. Strains insensitive to the temperature ($p > 0.05$) are highlighted in green, strains leading to minor changes in conductivity levels as the temperature increases (negative estimate, $p < 0.05$) are highlighted in blue, and strains displaying a warm-dependency (positive estimate, $p < 0.05$) are highlighted in red. The number of replicated experiments for each modality (strain x temperature condition) varied from 3 up to 27.